Electronic Spectroscopy of the Al−CH_4/CD_4 Complex

Irina Gerasimov, Jie Lei, and Paul J. Dagdigian*

Department of Chemistry, The Johns Hopkins University, Baltimore, Maryland 21218-2685

Received: March 24, 1999; In Final Form: May 24, 1999

The weakly bound Al−CH_4 complex, and the fully deuterated version, Al−CD_4, were prepared in a pulsed supersonic beam and probed with laser fluorescence excitation spectroscopy. Transitions to bound vibrational levels in electronic states correlating with the Al(5s,4d) + CH_4/CD_4 dissociation asymptotes have been observed. Resonance fluorescence from the excited levels could not be detected. Rather, these excited levels decay nonradiatively, and the excitation spectrum was obtained by monitoring emission from the lower Al atomic levels and AlH A → X chemiluminescence from formation of AlH($A^1\Pi$) within the excited complex. The band systems were dominated by progressions in the excited-state Al−CH_4/CD_4 van der Waals stretch vibrational mode. It was not possible to make unambiguous upper-state vibrational quantum number assignments, and lower bounds to excited-state binding energies were obtained. Band contour analysis of the AlH chemiluminescence spectra indicates that the excited AlH($A^1\Pi$) product is formed with approximately equal Λ-doublet populations, in contrast to the marked propensity for formation of e levels in the reactive decay of the Al(5s)−H_2 complex [Yang, X.; Dagdigian, P. J. *J. Chem. Phys.* **1998**, *109*, 8920].

1. Introduction

The interaction of the Al atom with methane has been of interest for some time. The reaction between these species within a cryogenic matrix has been studied with various techniques, including UV electronic, IR vibrational absorption, and EPR spectroscopies.[1,2] A photoreversible reaction, leading to the formation of CH_3AlH through an insertion mechanism, was found. The possible reaction pathways in this system have been investigated by quantum mechanical theoretical methods.[3] It was found that the lowest-energy CH_3AlH product can be reached from the reaction of ground-state atoms with methane through a high-barrier insertion process.

Study of the interaction of an Al atom with methane can be carried out through spectroscopic studies of isolated, weakly bound complexes of these species. There have been a number of such studies of complexes of metal atoms and ions with methane. Fluorescence excitation and multiphoton ionization spectra have been recorded and analyzed for the Hg−CH_4 complex.[4,5] Wallace and Breckenridge have observed predissociation products from electronic excitation of Cd−CH_4.[6] The rotational structure in the action spectrum was interpreted, and it was postulated that the complex could be described as a hindered rotor with η_3-coordination (C_{3v} symmetry) of the CH_4 molecule. Kleiber and co-workers[7,8] have probed electronic transitions in the ionic Mg^+−CH_4 and Ca^+−CH_4/CD_4 complexes through photodissociation spectroscopy. For the former, the action spectrum was structureless, and both nonreactive (Mg^+) and reactive (MgH^+, $MgCH_3^+$) products were observed. A structured spectrum was observed for the Ca^+ complexes, and excited-state stretch and bend vibrational frequencies were assigned. Brucat and co-workers[9] have studied the V^+−CH_4 complex through photodissociation spectroscopy and similarly assigned van der Waals stretch and bend frequencies.

The general theory for the vibration−rotation states of a van der Waals complex of a structureless atom and a spherical top, such as methane, has been elaborated by Hutson and Thornley[10] and Randall et al.[11] Heijmen et al.[12] have recently carried out a detailed theoretical study of the Ar−CH_4 complex. Ohshima and Endo[13] earlier described the correlation between the free rotor CH_4 and bending vibrational levels as a function of the strength of the lowest-order T_3 anisotropy, and they also observed the microwave spectrum of the CH_4−HCl complex. Infrared spectra of CH_4−rare gas complexes have been observed in the region of both the free C−H stretch[14−17] and bend[18] frequencies. Infrared spectra of SiH_4−rare gas complexes have also been reported.[19,20]

To our knowledge, the nonbonding interaction of the Al atom has not been investigated by quantum chemical calculations. The dissociation energy of the ionic Al^+−CH_4 complex has been reported[21] to equal 2120 ± 105 cm^{-1}. The binding energies, geometries, and vibrational frequencies of the Mg^+−CH_4 complex in several electronic states have been calculated by Bauschlicher and Sodupe.[22] The ground 3s state of the ion binds to methane with η_3-coordination, and the CH_4 moiety is not significantly distorted by the binding. Electron excitation to the 3p state is found to cause a significant change in the geometry of the complex, and the coordination is altered to η_2 in the most strongly bound electronic state ($^2B_1$) correlating with the Mg^+-(3p)−CH_4 asymptote.

To probe the two-body interaction between the Al atom and methane in both the ground and excited electronic states, we have carried out a study of the laser fluorescence excitation spectrum of weakly bound binary complexes of the Al atom with CH_4 and its fully deuterated isotopomer CD_4. This work represents an extension of our recent work on other weakly bound complexes containing the Al atom, including AlNe,[23] Al−H_2,[24] and Al−N_2.[25] We have investigated the electronic spectrum of the Al−CH_4/CD_4 complex in the region of the atomic transitions from the ground 3p state to the 5s and 4d Rydberg states. Similar to what we found for the corresponding states of Al−H_2 and Al−N_2, excited Al(5s,4d)−CH_4 does not decay radiatively but rather undergoes predissociation and chemical reaction, and we observe atomic Al 3d → 3p and 4s → 3p emission and AlH $A^1\Pi \rightarrow X^1\Sigma^+$ chemiluminescence. On the

10.1021/jp991001k CCC: $18.00
Published on Web 07/09/1999

basis of the above-described calculations on complexes of other metal atoms with methane, it is most likely the equilibrium geometry of the ground-state Al(3p)−CH_4 complex is the C_{3v} η_3-coordinated structure. As in the ground electronic state of aluminum atom−rare gas complexes,[23,26−28] the unpaired electron in Al(3p)−CH_4 should occupy the 3p component perpendicular to the Al−molecule axis to minimize the electron repulsion, leading to a ^{2}E ground state.

2. Experimental Section

The apparatus in which the laser fluorescence excitation spectra were recorded has been described in detail previously.[24,29−31] A supersonic beam containing Al atoms and weakly bound complexes of Al was produced in a pulsed free jet expansion (0.2 mm diam orifice) of mixtures of TMA (trimethylaluminum, obtained from Aldrich Chemical Co.) with CH_4 and He through 193 nm photolysis of TMA at the nozzle orifice. In some experiments, methane was replaced with CD_4 (99 atom %, obtained from Isotec).

Fluorescence excitation spectra were recorded 1.2−1.8 cm downstream of the nozzle using the frequency-doubled output of an XeCl excimer laser pumped dye laser (Lambda Physik) in the wavelength region near the Al atomic 5s ^{2}S ← 3p ^{2}P and 4d ^{2}D ← 3p ^{2}P transitions at 265.3 and 256.9 nm, respectively. The dye laser was operated in the low-resolution mode, yielding a spectral bandwidth of ∼0.3 cm^{-1}. Typical UV pulse energies for the recording of excitation spectra were 5−50 μJ in a 0.2 cm diameter beam.

The laser-induced fluorescence signal passed through a $^1/_4$ m monochromator employed without slits and was detected with a photomultiplier (EMI 9813QB), whose output was directed to a gated integrator and then to a computer. The monochromator was used to help discriminate the fluorescence signal from background light induced by the photolysis laser. In addition, the gain of the photomultiplier was switched off during the excimer laser pulse. Resolved fluorescence emission spectra were recorded with 250 μm slits installed in the monochromator (0.8 nm spectral resolution). The monochromator was operated in first order for detection of Al 4s → 3p emission (394.5 nm) and AlH A → X chemiluminescence (424−440 nm) and in second order for detection of 3d → 3p emission (308.3 nm).

A portion of the fundamental output of the dye laser was directed through a solid fused-silica Etalon (free spectral range 0.676 cm^{-1} in the visible) in order to provide wavenumber markers. Absolute calibration of the laser wavenumber was carried out using Al atomic transitions.

3. Results

3.1. The 5s ← 3p Transition. As in the case of the corresponding electronic transition in the Al−N_2 complex,[25] resonance fluorescence from radiative decay of the excited Al(5s)−CH_4 complex could not be detected. Rather, excitation spectra were recorded with good signal-to-noise ratio when the monochromator in the detection train was tuned to the 3d → 3p and 4s → 3p Al atomic transitions. This implies that this excited electronic state of the complex decays nonradiatively.

Figure 1 displays a laser fluorescence excitation spectrum of the Al−CH_4 complex for excitation wavenumbers slightly below that of the Al 5s ^{2}S ← 3p ^{2}P$_{1/2}$ atomic transition [37 689 cm^{-1} (ref 32)]. The spectra shown in panels a and b were recorded with the monochromator adjusted to transmit 3d → 3p (308.3 nm) and 4s → 3p (394.5 nm) emissions, respectively. Emission on the former transition was found to be approximately 60% stronger than on the latter (not corrected for the wavelength

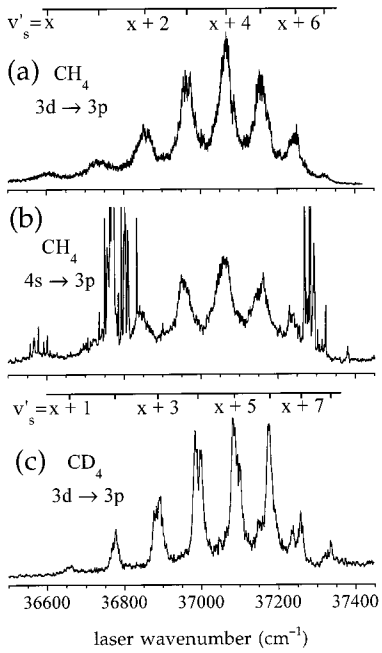

Figure 1. Laser fluorescence excitation spectra of a free jet containing Al atoms produced by 193 nm photolysis of TMA in pure CH_4 (panels a and b) and a CD_4 (2% mole fraction)−He mixture (panel c) at a total backing pressure of 8.8 atm. These spectra were recorded by monitoring Al atomic 3d → 3p (panels a and c) and 4s → 3p (panel b) emissions, as the excitation laser wavenumber was scanned. The Al−CH_4/CD_4 bands, which represent excitation to the 5s electronic state, are assigned to progressions in the Al−M van der Waals stretch mode. As discussed in the text, the absolute vibrational assignment could not be determined.

dependence of the detection sensitivity of the monochromator/photomultiplier combination). In addition to the broad features in both spectra, which are assigned below to the Al−CH_4 complex, additional, sharp, resolved features were present when the 4s → 3p emission was monitored, particularly in the wavenumber ranges 36 770−36 850 and 37 260−37 300 cm^{-1}.

Several complex and irregular bands of the AlH molecule have been reported in the wavenumber range 36 630−37 040 cm^{-1}. These bands have defied rotational analysis as the excited state appears to be perturbed and predissociated, while the corresponding bands in AlD have been assigned to a $^3\Pi$ ← a$^3\Pi$ transition.[33] The pattern of sharp lines seen in the present work is similar to that reported for AlH in this wavenumber range. These lines thus appear to involve the AlH molecule, which has previously been observed in supersonic beams containing photolyzed TMA,[34] and not the Al−CH_4 complex. Our observation of AlH lines by detection of emission from Al(4s) atoms also indicates that the excited state is predissociated. Formation of this excited atomic state is energetically allowed through optical excitation of AlH(a$^3\Pi$) in this wavenumber range. From the measured band origins of the b$^3\Sigma^-$ − a$^3\Pi$ and b$^3\Sigma^-$ − X$^1\Sigma^+$ transitions,[35,36] the a$^3\Pi$ state is computed to lie 15 557 cm^{-1} above the ground X$^1\Sigma^+$ state.

A progression of broad bands is clearly seen in the Al−CH_4 excitation spectrum displayed in Figure 1a. Essentially identical excitation spectra were observed with a wide range of CH_4 mole fractions in the seed gas, ranging from 8% to 100% (the balance being He). Moreover, these bands were seen only when TMA and CH_4 were present in the seed gas and the photolysis laser was on. We thus assign the carrier of these bands as the binary Al−CH_4 complex. The 5s ← 3p electronic transitions of weakly bound complexes of Al atoms with small molecules (M = H_2, N_2) have been found to be dominated by excited-state progres-

TABLE 1: Band Positions (cm^{-1}) for Transitions to van der Waals Stretch Excited Levels of Al(5s)−CH_4/CD_4[a]

v_s'	Al−CH_4	Al−CD_4
x[b]	36 600 (21)	
$x+1$	36 726 (21)	36 656 (10)
$x+2$	36 851 (17)	36 776 (6)
$x+3$	36 957 (16)	36 886 (8)
$x+4$	37 061 (13)	36 991 (6)
$x+5$	37 151 (12)	37 085 (6)
$x+6$	37 236 (12)	37 173 (5)
$x+7$	37 317 (8)	37 258 (6)
$x+8$		37 338 (11)

[a] Standard deviations of the band positions are given in parentheses. [b] Vibrational assignment not certain.

sions in the Al−M van der Waals stretching vibrational mode.[24,25] In these complexes, as well as AlRg (Rg = rare gas) complexes, excitation of the atom causes a large change in the binding energy and Al−M equilibrium atom−molecule separation and hence results in considerable Franck−Condon activity in the van der Waals stretch mode.[24−26] The series of bands of Al−CH_4 displayed in Figure 1a,b is similarly assigned to the Al−CH_4 stretch progression.

The Al−CH_4 bands displayed in Figure 1 are quite broad, and the rotational structure could not be resolved. However, the profiles cannot be fit to pure Lorentzian profiles. Thus, there is a significant heterogeneous component to the width, due to the rotational structure, within each band. The corresponding bands in the electronic spectrum of the Al−N_2 complex displayed partially resolved rotational structure, with Lorentzian line widths of the order of 0.5 cm^{-1}. The Al−CH_4 bands displayed in Figure 1a are consistent with Lorentzian line widths of the order of $\leq$20 cm^{-1}, implying an excited-state lifetime of $\geq$0.3 ps. Table 1 presents the transition wavenumbers of the bands, estimated as the wavenumber of the maximum intensity within each band.

The intensities of the bands in the stretch progression displayed in Figure 1a decrease as the excitation wavenumber is reduced. While the feature near 36 610 cm^{-1} is the lowest-energy band that can be positively identified in the spectrum, it is unclear whether it is the first member of the progression or whether lower-energy bands are not visible because of poor Franck−Condon factors. Thus, the van der Waals stretch vibrational quantum number v_s' of this band can only be given as $v_s' = x$, where $x \geq 0$.

In an attempt to assign the stretch quantum numbers, the excitation spectrum of the isotopically substituted Al−CD_4 complex was recorded. (It should be noted that Al has only one stable isotope, of amu 27.) The spectrum of Al−CD_4 is displayed in Figure 1c. As expected, a progression of bands, assigned to the van der Waals stretch mode, is observed, with the transition wavenumbers shifted from those of the Al−CH_4 bands. The widths of the Al−CD_4 bands are significantly smaller than those of Al−CH_4, with again a significant heterogeneous contribution to the broadening. The contours of the bands have variable shapes across the progression. Transition wavenumbers of the bands, estimated as the centroid, are reported in Table 1. We also see at the high wavenumber of Figure 1c evidence for activity in modes other than the van der Waals stretch mode.

In a diatomic complex, isotopic substitution of the atoms usually allows unambiguous assignment of the vibrational quantum numbers. The situation with atom−molecule complexes, i.e., Al−CH_4/CD_4, is not quite so simple. The transition wavenumber for the origin band of an electronic transition in the Al−CH_4 complex can be expressed as

$$T_{00} = T_e + G_0' - G_0'' \quad (1)$$

where T_e is the wavenumber difference between the minima of the Al(5s,3p)−CH_4 potential energy surfaces (PESs), and G_0'' and G_0' are the zero-point energies of the complex in its ground and excited electronic states, respectively. The excitation energy T_e is the same for the Al−CH_4 and Al−CD_4 complexes. To describe the energy of a band within the excited-state van der Waals stretch progression, we write the energy of the v_s' stretch level, relative to that of the excited-state zero-point level, as

$$G(v_s') = \omega_e' v_s' - \omega_e x_e' v_s'(v_s' + 1) \quad (2)$$

With eqs 1 and 2, the transition wavenumber for excitation to the v_s' stretch vibrational level from the ground vibronic level of a given isotopomer (i) of the Al−CH_4/CD_4 complex becomes

$$T^{(i)}(v_s',0) = T_{00} + \rho_i \omega_e' v_s' - \rho_i^2 \omega_e x_e' v_s'(v_s' + 1) + \Delta_i \quad (3)$$

The band origin T_{00} and the vibrational spectroscopic constants ω_e' and $\omega_e x_e'$ apply to the Al−CH_4 complex. The mass scaling factor ρ_i is defined as unity for Al−CH_4 and $[\mu(\text{Al}-\text{CH}_4)/\mu(\text{Al}-\text{CD}_4)]^{1/2} = 0.934\,938$ for Al−CD_4. The term Δ_i is defined to be zero for Al−CH_4 and for Al−CD_4 equals the following differences of zero-point energies:

$$\Delta_i(\text{Al}-\text{CD}_4) = [G_0'(\text{Al}-\text{CD}_4) - G_0'(\text{Al}-\text{CH}_4)] - [G_0''(\text{Al}-\text{CD}_4) - G_0''(\text{Al}-\text{CH}_4)] \quad (4)$$

This difference in the zero-point energies includes changes in the vibrational frequencies of all the intermolecular and intramolecular modes of the complex.

The binding energy, and hence the vibrational frequencies, are larger in the excited than in the ground electronic state of the complex. Moreover, the vibrational frequencies are larger for Al−CH_4 than for Al−CD_4. These considerations suggest that the quantity Δ_i(Al−CD_4) is negative. With this sign of Δ_i(Al−CD_4), the excited-state stretch vibrational quantum numbers v_s' for the bands in the Al−CD_4 excitation spectrum in Figure 1b have been correlated with those in Figure 1a, as indicated in the figure.

Assignment of the excited-state quantum numbers v_s' for an atom−molecule complex requires knowledge of the zero-point energy difference Δ_i since isotopic substitution affects more than one mode. In our study of the Al−N_2 complex,[25] we were able to estimate this quantity. Unfortunately, we have insufficient information to estimate Δ_i(Al−CD_4). Fitting the band positions reported in Table 1 to eq 3 with the assumption that $x = 0$ yields the following spectroscopic constants: $T_{00} = 36\,580 \pm 10$, $\omega_e' = 137.9 \pm 5.5$, $\omega_e x_e' = 3.88 \pm 0.59$, $\Delta_i = -37.7 \pm 5.2$ cm^{-1}. Performing this fit with higher assumed values of x yields smaller values for T_{00} and Δ_i and a larger value for ω_e'. It should be noted that the corresponding bands of Al−$^{14,15}N_2$ could be fit with the assumption that $x = 0$.[25]

Since we have not been able to obtain a definitive vibrational assignment for the bands displayed in Figure 1, we can give only a lower bound to the binding energy in the excited electronic state. From the displacement of the transition to the $v_s' = x$ band from the Al 5s ← 3p atomic transition, we obtain $D_0' - D_0'' \geq 1089$ cm^{-1}. Linear Birge−Sponer extrapolation with the above quoted vibrational constants yields a value of $37\,757 \pm 199$ cm^{-1} for the excitation energy of the dissociation limit. The quoted uncertainty is the uncertainty in D_e', estimated as $\omega_e'^2/4\omega_e x_e'$ for a Morse function. This excitation energy is approximately equal to the energy of the Al(5s) + CH_4

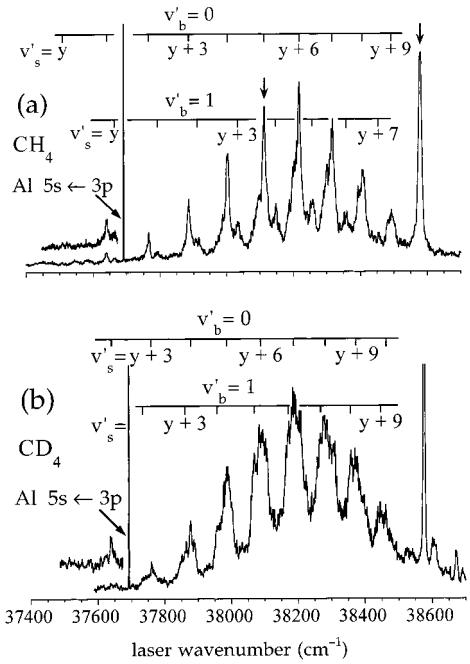

Figure 2. Laser fluorescence excitation spectra of a free jet containing Al atoms produced by 193 nm photolysis of TMA in a (a) CH_4 (8% mole fraction)−He and a (b) CD_4 (8% mole fraction)−He mixture at a total backing pressure of 8.2 atm. These spectra were recorded by monitoring the Al 3d → 3p emission as the excitation laser wavenumber was scanned. Bands assigned to the van der Waals stretch progression involving excitation of the most strongly bound Al(4d)−CH_4/CD_4 electronic state are indicated. As discussed in the text, the absolute vibrational assignment could not be determined. A second stretch progression in combination with one quantum of bending excitation is also denoted. As discussed in the text, the assignment of the bend−stretch combination bands is tentative. The isolated strong features near 38 600 cm^{-1} are assigned as excitation to another electronic state. The amplified portions of the spectra at low wavenumbers were recorded with higher probe laser energies. The vertical arrows in panel (a) indicate the bands for which AlH chemiluminescence spectra were recorded (see Figure 3).

asymptote and hence does not yield a useful estimate for the ground-state dissociation energy. Since the polarizability of CH_4 is slightly larger than that of N_2 [2.59 vs 1.74 Å^2 (ref 37)], the binding energy D_0''(Al−CH_4) should be comparable to or slightly greater than that of Al−N_2 [D_0''(Al−N_2) = 250−350 cm^{-1} (refs 25, 38, and 39)]. Setting D_0(Al−CH_4) = 400 cm^{-1}, the above quoted limit on the difference in dissociation energies implies that D_0'(Al−CH_4) ≥ 1489 cm^{-1}. The symmetry of this electronic state is assigned as $^2A_1$ since a single PES emanates from the Al(5s) + CH_4/CD_4 asymptote.

3.2. The 4d ← 3p Transition. For transition wavenumbers between those of the Al atomic 5s ^2S ← 3p $^2P_{1/2}$ and 4d ^2D ← 3p $^2P_{1/2}$ transitions, at 37 689 and 38 932 cm^{-1}, respectively,[32] a second set of bands assignable to the Al−CH_4/CD_4 complex was observed. Upon excitation of these bands, emission on the Al atomic 3d → 3p and 4s → 3p transitions, as well as AlH A → X chemiluminescence, was observed. These excitation spectra had approximately the same relative band intensities, and the ratio of the emission signals was 1:0.8:0.06 for the Al 3d → 3p line, the 4s → 3p line, and AlH chemiluminescence, respectively (not corrected for the wavelength dependence of the detection sensitivity). No emission from the lower Al 5s state was observed. Figure 2 presents fluorescence excitation spectra in this wavenumber region for both the Al−CH_4 and Al−CD_4 complexes. In both cases, Al 3d → 3p atomic emission was monitored while the excitation laser wavenumber was being scanned. Similar Al−CH_4 excitation spectra were recorded with monitoring of the Al atomic 4s → 3p emission and AlH chemiluminescence.

Progressions of bands are evident in the spectra displayed in Figure 2. The Al−CH_4 spectrum displays two obvious progressions. We assign the stronger of the two as an excited-state progression in the van der Waals stretch mode, as in the case of the 5s ← 3p transition, discussed in section 3.1, and in the analogous transition in Al−N_2.[25] We designate the stretch vibrational numbers of the upper levels of these bands as $\upsilon_s' = y, y + 1$, etc. The structure of these bands clearly changes through the progression. This could be the result of the vibrational dependence of the excited-state rotational constants. There is also a clear, weaker progression of bands displaced by 26 to 42 cm^{-1} to higher wavenumbers from the pure stretch bands. We assign the weaker bands as a progression of combination bands involving excitation of vibrational levels with van der Waals excitation and one quantum of van der Waals bend excitation, as indicated in Figure 2a, with a bending frequency $\omega_b' \approx 145$ cm^{-1}. Optical excitation of both the pure stretch and bend−stretch combination levels from the ground state is vibronically allowed. The enhanced 3d → 3p emission with irradiation of the Al 5s ← 3p atomic line is due to formation of Al(3d) atoms in bimolecular collisions involving excited Al(5s) atoms within the supersonic beam, as discussed previously.[25,40]

The spectrum of Al−CD_4 in Figure 2b displays a single obvious progression of broad features. In view of our observation that the bands involving the transition to the 5s electronic state are broader for Al−CH_4 than for Al−CD_4 (see Figure 1), it is surprising that the Al−CD_4 features in Figure 2b, involving the transition to the 4d electronic state, are broader than the Al−CH_4 bands in Figure 2a. The widths of the Al−CD_4 features in Figure 2b are not due to enhanced Lorentzian broadening, but rather the bands appear to be heterogeneously broadened, due to unresolved rotational structure and/or overlapping vibrational transitions.

With our assignment of a bending frequency of 145 cm^{-1} for the Al(4d)−CH_4 complex, we offer a possible explanation for the large width of the Al−CD_4 bands as arising from overlapping vibrational transitions. Since the van der Waals bending vibrational coordinate involves the motion of hydrogen atoms, CD_4 isotopic substitution should reduce the bending frequency by a factor of approximately $[m(H)/m(D)]^{1/2}$, or 0.707. These considerations lead to an estimate of ∼103 cm^{-1} for ω_b' of the Al−CD_4 complex. This further implies that the combination stretch−bend transitions with $\upsilon_b' = 1$ overlap the next higher pure stretch transition, as indicated in Figure 2b. One difficulty with this explanation is that Al−CD_4 bend−stretch combination bands would have to have intensities comparable to those of the pure stretch bands, while the former in Al−CH_4 are considerably weaker than the pure stretch bands (see Figure 2a).

We report in Table 2 estimated transition wavenumbers for bands of the pure stretch progressions of both Al−CH_4 and Al−CD_4. As with the electronic transition discussed in section 3.1, we cannot clearly identify the lowest-energy band of the pure stretch progressions in Figure 2 and hence cannot assign the upper-level stretch quantum numbers υ_s' in this way. We also attempted to make quantum number assignments from the observed isotope shifts. This was not successful since we have no estimate for Δ_i(Al−CD_4) for this electronic transition. Fitting the band positions reported in Table 2 to eq 3 and assuming that $y = 0$ yields the following spectroscopic constants: T_{00} =

TABLE 2: Band Positions (cm^{-1}) for Transitions to van der Waals Stretch Excited Levels of Al(4d)−CH_4/CD_4[a]

v_s'	Al−CH_4	Al−CD_4
y[b]	37 508 (8)	
$y+1$	37 639 (3)	
$y+2$	37 765 (6)	37 639 (14)
$y+3$	37 886 (7)	37 759 (14)
$y+4$	38 001 (9)	37 877 (16)
$y+5$	38 110 (12)	37 987 (12)
$y+6$	38 216 (8)	38 082 (16)
$y+7$	38 317 (10)	38 187 (17)
$y+8$	38 406 (12)	38 284 (17)
$y+9$	38 495 (10)	38 371 (12)
$y+10$		38 460 (9)

[a] Standard deviations of the band positions are given in parentheses. [b] Vibrational assignment not certain.

37510 ± 4, $\omega_e' = 132.9 \pm 2.6$, $\omega_e x_e' = 2.19 \pm 0.24$, $\Delta_i = -87.7 \pm 5.3$ cm^{-1}. Performing this fit with higher assumed values of y yields smaller values for T_{00} and Δ_i and a larger value for ω_e'. In the case of the Al−$^{14,15}N_2$ complex, the corresponding bands were fit with the assumption that $y = 9 \pm 1$.[25]

A lower bound to the binding energy in this excited electronic state can only be given since a definitive vibrational assignment for the bands displayed in Figure 2 has not been obtained. From the displacement of the transition to the $v_s' = y$ band from the Al 4d ← 3p atomic transition, we obtain $D_0' - D_0'' \geq 1424$ cm^{-1}. Linear Birge−Sponer extrapolation with the above quoted vibrational constants yields a value of 39 458 ± 238 cm^{-1} for the energy of the dissociation limit, and hence a ground-state dissociation energy of 526 ± 238 cm^{-1}. This value is within the range of the expected value for this quantity. Setting D_0(Al−CH_4) = 400 cm^{-1} as in section 3.1, the above quoted limit on the difference in dissociation energies implies that D_0'(Al−CH_4) ≥ 1824 cm^{-1}.

In addition to the van der Waals stretch progressions discussed above, there is a very strong feature near 38 600 cm^{-1} in the excitation spectra of both Al−CH_4 and Al−CD_4 shown in Figure 2. This feature displays only a very small isotope shift. Several electronic states of the complex can emanate from the degenerate atomic asymptote Al(4d) + CH_4/CD_4, as has been observed for AlRg complexes.[26] In these diatomic complexes, the binding energies have the ordering $^2\Delta > {}^2\Pi > {}^2\Sigma^+$, as expected from simple arguments concerning the minimization of nonbonding electron repulsion. One possibility is that the bands of Al−CH_4/CD_4 near 38 600 cm^{-1} involve excitation of a less strongly bound electronic state of the complex correlating to the Al(4d) + CH_4/CD_4 asymptote than does the state associated with the van der Waals stretch progression. A similar feature was observed in the electronic spectrum of the Al−N_2 complex, although its relative intensity was weaker than in the present system.[25] From the undeveloped vibrational structure, it would appear that there is not a significant change in geometry for excitation of this electronic state.

3.3. AlH Chemiluminescence Spectra. As with the previously studied Al−H_2 complex,[24] chemical reaction within the Al−CH_4 complex to yield electronically excited AlH($A^1\Pi$) products is energetically allowed. An additional chemical reaction pathway to form $AlCH_3$ products is possible for the Al−CH_4 complex.[3] Unfortunately, fluorescence from electronically excited $AlCH_3$ has not, to our knowledge, been observed, although the laser spectroscopic detection of $AlCH_3$ by resonance-enhanced multiphoton ionization has been reported.[41] The pure rotational spectrum of $AlCH_3$ has been recently observed.[42]

The threshold excitation energy T_{exc} of the Al−CH_4 complex for which formation of AlH($A^1\Pi$) products by chemical reaction within the complex is energetically allowed can be estimated as follows:

$$T_{exc} = D_0(H-CH_3) - D_0(AlH) + T_{00}(AlH) - D_0(Al-CH_4) \quad (5)$$

In eq 5, D_0(H−CH_3) and D_0(AlH) are bond dissociation energies (at 0 K), T_{00}(AlH) is the band origin wavenumber of the AlH $A^1\Pi \rightarrow X^1\Sigma^+$ transition, and D_0(Al−CH_4) is the binding energy of the complex in its ground electronic state. The bond dissociation energies and the AlH band origin wavenumber are available in the literature.[43−45] Employing the D_0(Al−CH_4) = 400 cm^{-1}, as discussed in section 3.1, we obtain a threshold energy T_{exc} of 34 550 cm^{-1}.

With the above estimated threshold energy, AlH chemiluminescence is energetically allowed for excitation of electronic transitions associated with both the atomic Al 5s ← 3p and 4d ← 3p transitions, reported in sections 3.1 and 3.2. Chemiluminescence was observed with excitation in both spectral regions. However, the chemiluminescence intensity with 5s ← 3p excitation was weak, and analyzable spectra could not be recorded.

To deduce the internal state distribution of the AlH product from chemical reaction within the Al(4d)−CH_4 complex, chemiluminescence spectra were recorded at 0.8 nm resolution for several excitation wavenumbers. The chemiluminescence signal was weak, and the spectra were recorded with high excitation laser pulse energies (500 μJ). Under these conditions, the excitation transition is in the saturation regime. Hence, the excited state is expected to have little alignment.

Figure 3 displays AlH chemiluminescence spectra for excitation of two bands within the 4d ← 3p transition. The Al−CH_4 bands chosen for study are indicated by arrows in Figure 2a. These include one member of the stretch progression and the intense, separate band at high transition wavenumbers. We recorded the chemiluminescence spectra of the strong $\Delta v = 0$ sequence of the AlH $A^1\Pi - X^1\Sigma^+$ band system,[45] and emission from $v' = 0$ and 1 excited vibrational levels was observed. While the monochromator resolution was not sufficient to resolve individual AlH rotational lines within each A − X band, emission within the individual rotational branches (P, Q, R) is distinguishable in the spectra. In the orbitally degenerate $A^1\Pi$ electronic state, each rotational level is split into a closely spaced pair of Λ-doublet levels of e and f symmetry.[46] The electronic wave function is symmetric (A′) and antisymmetric (A″) with respect to reflection in the plane of rotation for the e and f levels, respectively.[47]

In a $^1\Pi \rightarrow {}^1\Sigma^+$ transition, the excited e levels emit in the P and R branch, while the f levels emit in the Q branch. In the high-J limit, the emission from the f levels will be twice as strong as that from the e levels if the Λ-doublet populations are equal.[48] The spectra displayed in Figure 3 exhibit strong Q branches. This contrasts sharply with the chemiluminescence spectra observed for decay of the Al(5s)−H_2 complex, for which the Q branches were very weak, indicative of a Λ-doublet propensity for formation of AlH($A^1\Pi$) products in e levels.[24] In unpublished work, AlH($^1\Pi$) formed from chemical reaction within the Al(4d)−H_2 complex was also found to be produced mainly in e Λ-doublet levels.[49]

A band contour analysis of the (0,0) bands in the chemiluminescence spectra in Figure 3 was performed to estimate AlH($A^1\Pi$, $v' = 0$) rotational populations. We did not attempt to analyze the (1,1) band because of its weakness. For both spectra in Figure 3, the relative intensity of the (1,1) band implies that

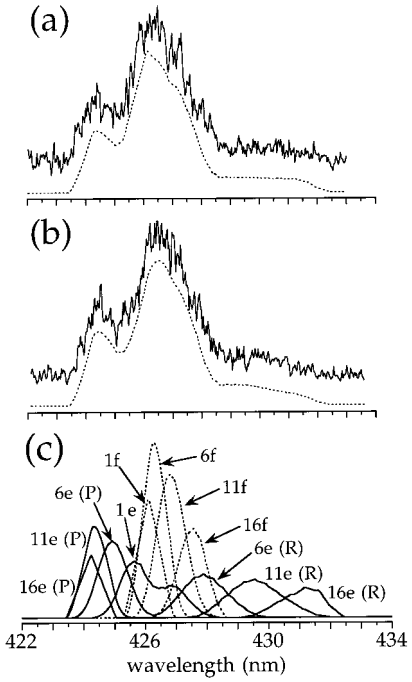

Figure 3. AlH $A^1\Pi-X^1\Sigma^+$ (0,0) band chemiluminescence spectra resulting from excitation of the Al−CH_4 bands at transition wavenumbers of (a) 38 118 and (b) 38 585 cm^{-1} (see Figure 2). The experimental spectra are drawn with solid lines, while computed spectra obtained from least-squares fits, as described in the text, are drawn with dotted lines. The spectral resolution was 0.8 nm. Panel c shows the basis functions employed in the least-squares fits describing the contributions to the spectra from each range of rotational levels fitted. The labels 1e, 1f, etc. designate the rotational level (angular momentum J and e/f symmetry label) defining the basis function. For e levels, emission in the P and R branches is separately identified.

the $v' = 1$ to $v' = 0$ vibrational population ratio is approximately 0.1. The AlH($A^1\Pi$) binding energy is small, and its potential energy curve has a barrier to dissociation.[48] Consequently, the higher rotational levels decay nonradiatively through rotational predissociation. The highest rotational level in $v' = 0$ that is bound and decays radiatively is $J' = 17$.[45] A different procedure was employed for the determination of the AlH($A^1\Pi$, $v' = 0$) rotational state distributions than was previously employed for analysis of the chemiluminescence spectra from the reactive decay of the Al(5s)−H_2 complex.[24] In the present study, we have employed a linear least-squares fitting procedure[50] to obtain the rotational populations. Since the populations of individual rotational levels of successive *J* values are strongly correlated with one another in such a fit, because of our limited spectral resolution, the population of every fifth *J* value in each Λ-doublet manifold was taken as an independent variable in the fit, with the populations of intervening levels determined by linear interpolation.

The derived AlH($A^1\Pi$, $v' = 0$) rotational state distributions obtained from fits to the chemiluminescence spectra displayed in Figure 3 are presented in Figure 4. Shown in Figure 3c are the basis functions employed in the least-squares fits. It can be seen that the basis functions for the 1f and 6f rotational levels are very similar, and this leads to a strong correlation in the derived populations for these levels. We see that the state distributions are similar for excitation of the two Al−CH_4 bands studied. The distributions are broad and cover the full range of radiating rotational levels. The relatively high derived population for the 1f level in Figure 4b could be the result of the correlation mentioned above. The rotational state distributions in Figure 4a,b have approximately equal e and f Λ-doublet populations;

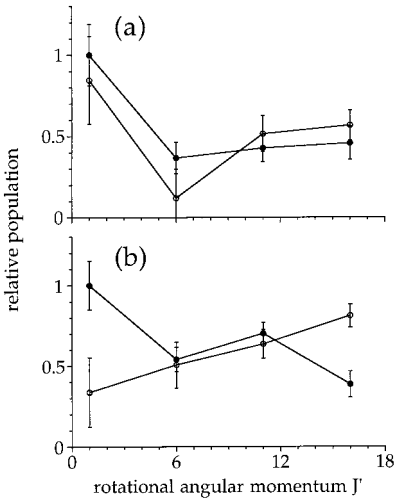

Figure 4. Derived AlH($A^1\Pi$, $v' = 0$) rotational state distributions from linear least-squares fits to the chemiluminescence spectra reported in Figure 3. The Al−CH_4 excitation energies were 38 118 and 38 585 cm^{-1} for panels a and b. The relative populations (with one σ error bars) are indicated with solid circles for e levels and with open circles for f levels. As described in the text, the population of every fifth rotational level in the two Λ-doublet manifolds were allowed to vary, and the populations of the intervening levels were computed by linear interpolation.

TABLE 3: Comparison of Binding Energies (cm^{-1}) of Various Al−M Complexes

M	α(M) ($Å^2$)[a]	D_0(Al(5s)−M)	D_0(Al(4d)−M)[c]	D_0(Al^+−M)
Ne	0.40	81[d]		
Ar	1.64	692[e]	787[e]	982.3 ± 5[e]
Kr	2.48	1216[e]	1429[e]	1528.5 ± 2[e]
H_2	0.81	300^{+160}_{-10}[f]		472 ± 52[g]
N_2	1.74	1218 ± 10[h]	2705 ± 165[h]	1924 ± 175[i]
	2.20[b]			
CH_4	2.60	≥1489[j]	≥1824[j]	2120 ± 105[g]

[a] Reference 37. [b] Second value for N_2 is $\alpha_{\|}$. [c] Dissociation energy for the most strongly bound electronic state correlating with the Al(4d) + M asymptote. [d] Reference 23. [e] Reference 26. [f] Reference 24. [g] Reference 21. [h] Reference 25. [i] Bouchard, F.; McMahon, T. Unpublished; cited in ref 39. [j] This work.

for both these distributions the integrated e to f population ratios are 1:0.9. The rotational state distributions from the reactive decay of excited Al(5s)−H_2 complexes are quite different from those reported in Figure 4. For reaction within Al(5s)−H_2, a strong preference for Λ-doublets of e symmetry, with a narrow state distribution peaking at $J' \approx 11$, was found.[24] The mean rotational excitation of the AlH($A^1\Pi$) products from reaction with Al(5s)−CH_4 excited complexes was much less than for Al(5s)−H_2 complexes.

4. Discussion

It is of interest to compare the binding energies of the AlRg and Al−molecule complexes that have been studied. Table 3 presents such a comparison for excited electronic states correlating with the Al(5s,4d) + M asymptotes. Since there are several electronic states emanating from the dissociation asymptote for the Al(4d)−M complexes, the binding energy for the most strongly bound state [$^2\Delta$ for AlRg complexes] is given in Table 3.

Also included in Table 3 are the polarizabilities of the atomic or molecular ligand. The major contribution to the long-range attractive interaction is usually the dispersion interaction, which scales with the polarizabilities of the interacting species.[51] The

equilibrium interparticle separation, and hence the binding energy, is actually governed by the balance between the attractive forces and the repulsion between the overlapping electron distributions. We see from Table 3 that there is a strong correlation between the magnitudes of the binding energies and the polarizabilities. This suggests that the range at which electron repulsion becomes significant is similar for these complexes.

For N_2, we have included both the isotropic polarizability α and the parallel component $\alpha_{||}$. Both quantum chemical calculations[38] and the rotational contours of bands in the fluorescence excitation spectrum[25] indicate that the Al−N_2 complex has a linear geometry. Thus, the parallel component may be the more appropriate quantity to consider in judging the strength of the Al−N_2 attractive interaction. Indeed, there is in this case a better correlation of the Al(5s)−N_2 binding energy with the binding energies of other Al(5s)−M complexes. However, N_2 has a large permanent quadrupole moment [-1.5×10^{-26} esu (ref 37)] so that there are both dispersion and induction contributions to the long-range Al−N_2 interaction energy.

The major uncertainty in this correlation arises from the lack of a definitive vibrational quantum number assignment for the Al−CH_4 bands reported in this study. It is possible that the Al(5s)−CH_4 binding energy could be significantly greater than that presented in Table 3. We also see in Table 3 that the Al(4d)−N_2 binding energy is significantly greater than expected. As we discussed previously, this could be an indication of the role of dative bonding in enhancing the strength of the attractive interaction, as was documented for BAr($C^2\Delta$).[31,52]

Also included in Table 3 are dissociation energies of the corresponding ionic Al^+−molecule complexes. It is expected that the dissociation energies of Rydberg states of neutral Al−molecule complexes at high *n* should approach those of the corresponding ionic complexes. In an extensive study of AlAr and AlKr Rydberg states, Heidecke et al.[26] found that the dissociation energies of high-*n* states did approach the binding energies of the corresponding ions. As in the case of the AlRg complexes, the binding energy of the Al(5s)−H_2 complex is less than that of the ionic Al^+−H_2 complex. It can be seen for Al−N_2 that the dissociation energy of the 5s state is less than that of the ion, while that of the 4d state is greater, as has been discussed previously.[25] The reported lower bounds for the binding energies of the 5s and 4d states of Al−CH_4 are less than the binding energy of Al^+−CH_4.

We noted in section 3.1 that the widths of the Al(5s)−CD_4 bands are significantly less than for Al(5s)−CH_4. This implies that the predissociation rates for this isotopomer are greater than for the deuterated species. We see in Figure 2 that the Al(4d)−CD_4 bands are, by contrast, broader than the corresponding Al−CH_4 bands. However, it is very likely that the Al(4d)−CD_4 features consist of overlapping vibrational transitions, and hence a raw comparison of the widths is not definitive.

The excited states can decay by either nonreactive predissociation to form a lower Al atomic state, as can be detected for formation of the Al(4s,3d) states by emission lines to the Al 3p ground state, or by chemical reaction within the excited complex. The rate of the latter process is governed by the motion of a hydrogen atom and should be slowed by deuteration. However, to judge by the weakness of the AlH chemiluminescence signal, chemical reaction is not the dominant mode of decay. It might also be expected that nonreactive predissociation, which depends on the nonadiabatic coupling of Al−CH_4 PESs, will be enhanced by hydrogen motions that lead to nonsymmetrical nuclear geometries. In contrast to AlRg complexes,[23,25,27,28] predissociation in excited Al−molecule complexes is found to lead to observable Lorentzian broadening.[24,25]

The rotational/Λ-doublet state distribution of AlH($A^1\Pi$) products from the reactive decay of Al(4d)−CH_4 complexes is quite different from that previously determined for the reactive decay of Al(5s)−H_2 complexes.[24] In the latter case, the AlH products were formed predominantly in e Λ-doublet levels, which have A′ symmetry with reflection of the wave function through the plane of rotation. This propensity was believed to be a consequence of the A′ symmetry of the Al(5s) + H_2 PES on which the reagents approach each other. As mentioned in section 3.3, a propensity to form AlH products of A′ symmetry is also found in the case of chemical reaction within Al(4d)−H_2 complexes.[49] This suggests that the excited AlH_2 electronic state accessed also has *A′* symmetry. The approach of Al(4d) and H_2 reagents yields PESs of both *A′* and *A″* symmetry, and it should be noted that the equilibrium geometries of the ground Al(3p)−H_2 state[53,54] and of the Al^+−H_2 ion,[21] and hence of Al−H_2 neutral Rydberg states, are T-shaped. The preferential Λ-doublet population in the AlH($A^1\Pi$) products from the decay of excited Al(5s,4d)−H_2 complexes reflects the fact that the plane of the triatomic complex and the plane of rotation of the AlH diatom should nearly coincide.

In the case of the Al(4d)−CH_4 complex, no such dramatic Λ-doublet propensity is observed, and the e to f population ratio is approximately unity. This lack of a propensity could arise from several factors. The most important consideration is probably the fact that the Al−CH_4 complex is nonplanar so that the plane of rotation of the AlH($A^1\Pi$) product is not well-defined with respect to any possible planes of symmetry in the complex. In addition, there are three possible hydrogen atoms that can be abstracted. Finally, in C_{3v} geometry, appropriate to Franck−Condon excitation from the ground state, the most strongly bound Al(4d)−CH_4 electronic state is orbitally degenerate, and the symmetries with respect to reflection through the σ_v planes are not well-defined.

Acknowledgment. This research was supported by the U.S. Air Force Office of Scientific Research under Grant No. F49620-98-1-0187. We gratefully acknowledge the assistance and advice of Xin Yang.

References and Notes

(1) Parnis, J. M.; Ozin, G. A. *J. Am. Chem. Soc.* **1986**, *108*, 1699.
(2) Parnis, J. M.; Ozin, G. A. *J. Phys. Chem.* **1989**, *93*, 1204.
(3) Yu, H.; Goddard, J. D. *Can. J. Chem.* **1989**, *68*, 633.
(4) Fuke, K.; Saito, T.; Nonose, S.; Kaya, K. *J. Chem. Phys.* **1987**, *86*, 4745.
(5) Duval, M.-C.; Soep, B. *Chem. Phys. Lett.* **1987**, *141*, 225.
(6) Wallace, I.; Breckenridge, W. H. *J. Chem. Phys.* **1992**, *97*, 2318.
(7) Cheng, Y. C.; Chen, J.; Ding, L. N.; Wong, T. H.; Kleiber, P. D.; Liu, D.-K. *J. Chem. Phys.* **1996**, *104*, 6452.
(8) Chen, J.; Cheng, Y. C.; Kleiber, P. D. *J. Chem. Phys.* **1997**, *106*, 3884.
(9) Hayes, T.; Bellert, D.; Buthelezi, T.; Brucat, P. J. *Chem. Phys. Lett.* **1997**, *264*, 220.
(10) Hutson, J. M.; Thornley, A. E. *J. Chem. Phys.* **1994**, *100*, 2505.
(11) Randall, R. W.; Ibbotson, J. B.; Howard, B. J. *J. Chem. Phys.* **1994**, *100*, 7042.
(12) Heijmen, T. G. A.; Wormer, P. E. S.; van der Avoird, A.; Miller, R. E.; Moszynski, R. *J. Chem. Phys.* **1999**, *110*, 5639.
(13) Ohshima, Y.; Endo, Y. *J. Chem. Phys.* **1990**, *93*, 6256.
(14) McKellar, A. R. W. *Faraday Discuss. Chem. Soc.* **1994**, *97*, 69.
(15) Lovejoy, C. M.; Nesbitt, D. J. *Faraday Discuss. Chem. Soc.* **1994**, *97*, 175.
(16) Block, P. A.; Miller, R. E. *Faraday Discuss. Chem. Soc.* **1994**, *97*, 177.
(17) Miller, R. E.; Heijmen, T. G. A.; Wormer, P. E. S.; van der Avoird, A.; Moszynski, R. *J. Chem. Phys.* **1999**, *110*, 5651.

(18) Pak, I.; Roth, D. A.; Hepp, M.; Winnewisser, G.; Scouteris, D.; Howard, B. J.; Yamada, K. M. T. *Z. Naturforsch.* **1998**, *53A*, 725.
(19) Randall, R. W.; Ibbotson, J. B.; Howard, B. J. *J. Chem. Phys.* **1994**, *100*, 7051.
(20) Brookes, M. D.; Hughes, D. J.; Howard, B. J. *J. Chem. Phys.* **1997**, *107*, 2738.
(21) Kemper, P. R.; Bushnell, J.; Bowers, M. T.; Gellene, G. I. *J. Phys. Chem. A* **1998**, *102*, 8590.
(22) Bauschlicher, C. W.; Sodupe, M. *Chem. Phys. Lett.* **1993**, *214*, 489.
(23) Yang, X.; Dagdigian, P. J.; Alexander, M. H. *J. Chem. Phys.* **1998**, *108*, 3522.
(24) Yang, X.; Dagdigian, P. J. *J. Chem. Phys.* **1998**, *109*, 8920.
(25) Yang, X.; Gerasimov, I.; Dagdigian, P. J. *Chem. Phys.* **1998**, *239*, 207.
(26) Heidecke, S. A.; Fu, Z.; Colt, J. R.; Morse, M. D. *J. Chem. Phys.* **1992**, *97*, 1692.
(27) McQuaid, M. J.; Gole, J. L.; Heaven, M. C. *J. Chem. Phys.* **1990**, *92*, 2733.
(28) Fu, Z.; Massick, S.; Kaup, J. G.; Benoist d'Azy, O.; Breckenridge, W. H. *J. Chem. Phys.* **1992**, *97*, 1683.
(29) Yang, X.; Hwang, E.; Dagdigian, P. J.; Yang, M.; Alexander, M. H. *J. Chem. Phys.* **1995**, *103*, 2779.
(30) Yang, X.; Hwang, E.; Dagdigian, P. J. *J. Chem. Phys.* **1996**, *104*, 599.
(31) Yang, X.; Dagdigian, P. *J. Chem. Phys.* **1997**, *106*, 6596.
(32) Moore, C. E. *Atomic Energy Levels, NSRDS-NBS 35*; U.S. Government Printing Office: Washington, DC, 1971; Vol. 1.
(33) Kleman, B. *Ark. Fys.* **1953**, *6*, 407.
(34) Hwang, E.; Dagdigian, P. J. *J. Chem. Phys.* **1995**, *102*, 2426.
(35) Challacombe, C. N.; Almy, G. M. *Phys. Rev.* **1937**, *51*, 930.
(36) Zhu, Y. F.; Shehadeh, R.; Grant, E. R. *J. Chem. Phys.* **1992**, *97*, 883.
(37) Gray, C. G.; Gubbins, K. E. *Theory of Molecular Fluids. Vol. 1: Fundamentals*; Clarendon Press: Oxford, U.K., 1984.
(38) Chaban, G.; Gordon, M. S. *J. Chem. Phys.* **1997**, *107*, 2160.
(39) Brock, L. R.; Duncan, M. A. *J. Phys. Chem.* **1995**, *99*, 16571.
(40) Dagdigian, P. J.; Yang, X. *Faraday Discuss.* **1997**, *108*, 287.
(41) Zhang, Y.; Stuke, M. *Jpn. J. Appl. Phys.* **1988**, *27*, L1349.
(42) Robinson, J. S.; Ziurys, L. M. *Astrophys. J.* **1996**, *472*, L131.
(43) Berkowitz, J.; Ellison, G. B.; Gutman, D. *J. Phys. Chem.* **1994**, *98*, 2744.
(44) Bauschlicher, C. W.; Langhoff, S. R. *J. Chem. Phys.* **1988**, *89*, 2116.
(45) Ram, R. S.; Bernath, P. F. *Appl. Opt.* **1996**, *35*, 2879.
(46) Brown, J. M.; Hougen, J. T.; Huber, K.-P.; Johns, J. W. C.; Kopp, I.; Lefebvre-Brion, H.; Merer, A. J.; Ramsay, D. A.; Rostas, J.; Zare, R. N. *J. Mol. Spectrosc.* **1975**, *55*, 500.
(47) Alexander, M. H.; Andresen, P.; Bacis, R.; Bersohn, R.; Comes, F. J.; Dagdigian, P. J.; Dixon, R. N.; Field, R. W.; Flynn, G. W.; Gericke, K.-H.; Grant, E. R.; Howard, B. J.; Huber, J. R.; King, D. S.; Kinsey, J. L.; Kleinermanns, K.; Kuchitsu, K.; Luntz, A. C.; MacCaffery, A. J.; Pouilly, B.; Reisler, H.; Rosenwaks, S.; Rothe, E.; Shapiro, M.; Simons, J. P.; Vasudev, R.; Wiesenfeld, J. R.; Wittig, C.; Zare, R. N. *J. Chem. Phys.* **1988**, *89*, 1749.
(48) Herzberg, G. *Molecular Spectra and Molecular Structure I. Spectra of Diatomic Molecules*, 2nd ed.; D. Van Nostrand: Princeton, NJ, 1950.
(49) Yang, X. Unpublished work.
(50) Press: W. H.; Flannnery, B. P.; Teukolsky, S. A.; Vetterling, W. T. *Numerical Recipes: The Art of Scientific Computing*; Cambridge University Press: New York, 1989.
(51) Stone, A. J. *Theory of Intermolecular Forces*; Clarendon Press: Oxford, U.K., 1996.
(52) Sohlberg, K.; Yarkony, D. R. *J. Phys. Chem. A* **1997**, *101*, 3166.
(53) Partridge, H.; Bauschlicher Jr., C. W.; Visscher, L. *Chem. Phys. Lett.* **1995**, *246*, 33.
(54) Chaban, G.; Gordon, M. S. *J. Phys. Chem.* **1996**, *100*, 95.